

Towards Good Practices in Evaluating Transfer Adversarial Attacks

Zhengyu Zhao^{†,*1}, Hanwei Zhang^{*,2} Renjue Li^{*,3,4}
 Ronan Sicre² Laurent Amsaleg⁵ Michael Backes¹

¹CISPA Helmholtz Center for Information Security ²LIS - Ecole Centrale Marseille

³SKLCS, Institute of Software, CAS ⁴University of Chinese Academy of Sciences

⁵Inria, Univ Rennes, CNRS, IRISA

{zhengyu.zhao,director}@cispa.de, {hanwei.zhang,ronan.sicre}@lis-lab.fr

lirj19@ios.ac.cn, laurent.amsaleg@irisa.fr

Abstract

Transfer adversarial attacks raise critical security concerns in real-world, black-box scenarios. However, the actual progress of attack methods is difficult to assess due to two main limitations in existing evaluations. First, existing evaluations are unsystematic and sometimes unfair since new methods are often directly added to old ones without complete comparisons to similar methods. Second, existing evaluations mainly focus on transferability but overlook another key attack property: stealthiness. In this work, we design good practices to address these limitations. We first introduce a new attack categorization, which enables our systematic analyses of similar attacks in each specific category. Our analyses lead to new findings that complement or even challenge existing knowledge. Furthermore, we comprehensively evaluate 23 representative attacks against 9 defenses on ImageNet. We pay particular attention to stealthiness, by adopting diverse imperceptibility metrics and looking into new, finer-grained characteristics. Our evaluation reveals new important insights: 1) Transferability is highly contextual, and some white-box defenses may give a false sense of security since they are actually vulnerable to (black-box) transfer attacks; 2) All transfer attacks are less stealthy, and their stealthiness can vary dramatically under the same L_∞ bound. Our code and a list of categorized attacks are publicly available at <https://github.com/ZhengyuZhao/TransferAttackEval>.

1. Introduction

Deep Neural Networks (DNNs) have achieved great success in various machine learning tasks. However, they are known to be vulnerable to *adversarial attacks*, which in-

entionally perturb model inputs to induce prediction errors [4, 66]. Adversarial attacks have been explored in white-box scenarios to evaluate worst-case model robustness as well as the black-box scenarios to understand real-world adversarial threats.

Black-box attacks can be divided into query-based and transfer-based attacks. Query-based [6, 11, 12, 23, 28] attacks need to sequentially query the target model multiple times. Since these queries are near-duplicates, the attack is easy to expose by simply monitoring the query history [13]. In a more realistic scenario, transfer attacks can work without accessing the target model but only transfer their adversarial effects from a local surrogate model. As a result, studying transfer attacks is more appropriate to understand real-world adversarial threats.

However, we find that existing evaluations of transfer attacks are limited in two main aspects. First, existing evaluations are often *unsystematic* and sometimes even *unfair*. Specifically, existing evaluations often simply add new attack methods to old ones to achieve the best transferability but with limited comparisons to similar methods. Even when similar methods are compared, existing evaluations sometimes lack fair hyperparameter settings (see details in Section 6). In addition, existing evaluations mainly focus on relatively simple attack settings involving only standard target models and weak defenses, such as the FGSM-based adversarial training [70]). Second, existing evaluations mainly focus on the attack strength, i.e. *transferability*, but largely overlook another key attack property: *stealthiness*. Specifically, the stealthiness is addressed only by the L_p -based imperceptibility of image perturbations. Using only L_p norms may be sufficient for evaluating white-box attacks but becomes less meaningful when larger perturbations are required [60, 68], as in transfer attacks. In particular, a recent study [14] notices that the transferability of L_∞ -bounded attacks is actually highly correlated with the L_∞ norms of their image perturbations. Moreover, other stealthiness

*Equal contribution

†Corresponding author

measures beyond imperceptibility are not well explored.

In this work, we address the above limitations by designing good practices in evaluating transfer adversarial attacks. We first introduce a new attack categorization to systematically and fairly analyze similar attack methods following specific criteria in each category. Our analyses lead to new findings that complement or even challenge existing knowledge. For example, we find that for input augmentation attacks, the early attack method Diversity Input (DI)-FGSM [84] surprisingly outperforms all subsequent methods by a large margin when they are compared fairly with the same number of input copies. Furthermore, we present a comprehensive evaluation of 23 representative attacks against 9 defenses on 5000 ImageNet images. In particular, we pay large attention to attack stealthiness, by adopting five diverse imperceptibility metrics beyond the L_p norms and also deeply investigating the finer-grained characteristics of the perturbation and misclassification.

Our evaluation results lead to new important insights: Regarding transferability, the optimal attack performance against one specific defense may not generalize to another. In particular, some defenses may largely overfit to the attacks that are used in defense optimization. For example, DiffPure [52], which claims high white-box robustness, is actually vulnerable to (black-box) transfer attacks with robust perturbations. Regarding stealthiness, *all* transfer attacks are indeed less imperceptible than the baseline PGD attack. Moreover, attacks under the same L_∞ bound yield dramatically different imperceptibility scores and finer-grained stealthiness characteristics.

2. Threat Model

Adversarial attacks on image classification can be briefly formulated as follows. Given a classifier $f(x) : x \in \mathcal{X} \rightarrow y \in \mathcal{Y}$ that predicts a label y for an original image x , an adversary generates an adversarial image x' by perturbing x . Following the common practice [5, 8, 53], we specify our threat model from three dimensions: adversary’s knowledge, adversary’s goal, and adversary’s capability,

2.1. Adversary’s Knowledge

An adversary can have various levels of knowledge about the target model. In the ideal, white-box scenario, an adversary has full control over the target model. In the realistic, black-box scenario, an adversary has either query access to the target model or in our transfer setting, no access but can only leverage a surrogate model. In this work, we focus on the most common transfer setting in which the surrogate and target models are trained on the same public dataset (here ImageNet) but with different architectures. Note that there are also a few studies exploring cross-dataset transferability [50, 96], which is beyond the scope of this work.

2.2. Adversary’s Goal

An adversary focuses on one of two types of misclassification: *untargeted* or *targeted*. An untargeted attack aims to fool the classifier into predicting any incorrect class other than the original one, i.e. $f(x') \neq y$. A targeted attack aims at a specific incorrect class t , i.e. $f(x') = t$. The targeted goal is strictly more challenging because a specific (target) direction is required, while many (including random) directions suffice for untargeted success. In this work, we follow most existing work to focus on the untargeted goal since targeted transferability remains an open problem [49, 100]. Beyond misclassification, we further consider a fine-grained metric that reports the ranking position of the true class in the target model’s prediction list.

2.3. Adversary’s Capability

In practice, the capability of an adversary should be the constraint of staying stealthy. Most existing research addresses this constraint by pursuing small, imperceptible image perturbations following specific metrics: typically L_p norms [9, 22, 36, 53, 67] but sometimes other metrics [1, 15, 33, 46, 56, 78, 81, 94, 99]. In this work, we follow the common practice to impose the L_∞ norm bound to achieve imperceptible perturbations. Moreover, we measure the perturbation size based on more advanced perceptual metrics. Beyond imperceptibility, we further look into other aspects of attack stealthiness, such as perturbation characteristics and misclassification characteristics. Note that there are also other recent studies exploring the transferability of “perceptible yet stealthy” adversarial images [3, 59, 98], which is beyond the scope of this work.

It is worth noting that the constraint on the attack budget is also important. In particular, unreasonably limiting the iteration number of attacks is shown to be one of the major pitfalls in evaluating adversarial robustness [8, 69, 100]. In this work, to avoid this problem, we ensure attack convergence by using enough iterations for iterative attacks and training epochs for generative attacks.

3. New Attack Categorization

In this section, we categorize transfer attacks into five categories: gradient stabilization, input augmentation, feature disruption, surrogate refinement, and generative modeling. These five categories are *disjoint*, i.e., each attack falls into *only one* category according to its core working mechanism. In this way, attacks that share the same working mechanism can be systematically compared along a single dimension with other factors fairly controlled. In contrast, existing work often combines attack methods from different categories for the best transferability but lacks systematic comparisons of similar attacks in the same category. Note that our categorization does not include the surrogate en-

semble attacks [39, 43] since they are generally applicable and normally require multiple surrogate models.

3.1. Gradient Stabilization Attacks

Different DNN model architectures tend to yield radically different decision boundaries, yet similar test accuracy, due to their high non-linearity [43, 62]. For this reason, the attack gradients calculated on a specific model may cause the adversarial images to trap into local optima, resulting in low transferability to another, unseen model. To address this issue, several studies adopt popular machine learning techniques for stabilizing iterative gradient updates. Specifically, a momentum term can be integrated into the attack optimization to accumulate previous gradients [17], and a Nesterov accelerated gradient (NAG) term can be integrated to look ahead [42]. The property of NAG is later examined in [74], where using only the last gradient is found to be better than using all previous gradients.

3.2. Input Augmentation Attacks

Learning adversarial images that can transfer to unseen models follows a similar principle to learning models that can generalize to unseen test images [40]. For this reason data augmentation, as a common technique for improving model generalizability, is exploited to improve attack transferability. To this end, several studies force the adversarial effects to be invariant to certain semantic-preserving image transformations, such as geometric transformations (e.g., resizing & padding [84] and translation [18]), pixel value scaling [42], random noise [72], and mixed images from other classes [73]. Several recent studies also explore more complex methods that refine the above transformations [89, 104], leverage regional (object) information [7, 38, 77], or rely on frequency-domain image transformations [45].

3.3. Feature Disruption Attacks

Conventional attacks naturally adopt the output-level, cross-entropy (CE) loss since they aim at misclassification. However, the output-level information is often model-specific. In contrast, features extracted from DNN intermediate layers are known to be more generic [35, 88]. Inspired by this fact, several studies propose to improve attack transferability based on feature disruptions. The general objective is to modify the image such that its feature is pushed away from the original feature. Specifically, early attacks treat all features indiscriminately [21, 27, 37, 44, 51, 102], which is shown to cause sub-optimal attack transferability because the model decision may only depend on a small set of important features [101]. For this reason, later attacks [76, 80, 95] instead calculate the feature distance only on important features that are computed based on model interpretability techniques [58, 64]. Feature disruption is also

explored for targeted attacks, where the image is modified such that its feature becomes more similar to a target image [32] or image distribution [30, 31].

3.4. Surrogate Refinement Attacks

The current CNN models are commonly optimized towards high prediction accuracy but with much less attention given to transferable representations. Several recent studies find that adversarial training can help pre-trained models better transfer to downstream tasks, although it inevitably trades off model accuracy in the source domain [16, 57, 71]. This finding encourages researchers to explore how the attack transferability can be improved based on refining the surrogate model in diverse aspects, such as training procedures [63, 86, 93], local architectures [79, 103], and activation functions [24, 91, 103]. This line of research also leads to rethinking the relation between the accuracy of the surrogate model and the transferability [93, 103].

3.5. Generative Modeling Attacks

In addition to the above iterative attacks, existing work also uses generative models to improve transferability. Basically, an image generator is learned on additional data such that it can take as input any original image and outputs an adversarial image with only one forward pass. During training, the generator is optimized to fool a discriminator, which is a pre-trained fixed classifier. Specifically, the earliest generative attack [54] adopts the widely-used cross-entropy loss. Later studies improve it by adopting a relativistic cross-entropy loss [50] or intermediate-level, feature losses [34, 96]. In particular, to improve targeted transferability, class-specific [49] and class-conditional [87] generators are also explored. In general, a clipping operation is applied during training to constrain the perturbation size.

4. Evaluation Methodology

In this section, we present data, models, attack/defense methods, as well as evaluation metrics for transferability and stealthiness.

4.1. Evaluation Settings

Data and models. We focus our evaluation on the challenging dataset ImageNet, because attack transferability on small datasets (e.g., MNIST and CIFAR) has been well solved [32], and it is interesting to explore the visual characteristics of large-resolution (adversarial) images. We consider four different model architectures: Inception-V3 [65], ResNet-50 [25], DenseNet-121 [26], and VGGNet-19 [61]. We randomly select 5000 images (5 per class¹) from the validation set that are correctly classified by all the above four models. All original images are resized and then cropped

¹Several classes contain fewer than 5 eligible images.

Table 1. Overview of the selected attacks.

Gradient Stabilization	Input Augmentation	Feature Disruption	Surrogate Refinement	Generative Modeling
MI [17] (CVPR’18)	DI [84] (CVPR’19)	TAP [102] (ECCV’18)	SGM [79] (ICLR’20)	GAP [54] (CVPR’18)
NI [42] (ICLR’20)	TI [18] (CVPR’19)	AA [32] (CVPR’19)	LinBP [24] (NeurIPS’20)	CDA [50] (NeurIPS’19)
PI [74] (BMVC’21)	SI [42] (ICLR’20)	ILA [27] (ICCV’19)	RFA [63] (NeurIPS’21)	TTP [49] (ICCV’21)
	VT [72] (CVPR’21)	FIA [76] (ICCV’21)	IAA [103] (ICLR’22)	GAPF [34] (NeurIPS’21)
	Admix [73] (ICCV’21)	NAA [95] (CVPR’22)	DSM [86] (arXiv’22)	BIA [96] (ICLR’22)

Table 2. Overview of the selected defenses.

Input Pre-processing	Purification Network	Adversarial Training
BDR [85] (NDSS’18)	HGD [41] (CVPR’18)	AT _∞ [83] (CVPR’19)
PD [55] (CVPR’18)	NRP [48] (CVPR’20)	FD _∞ [83] (CVPR’19)
R&P [82] (ICLR’18)	DiffPure [52] (ICML’22)	AT ₂ [57] (NeurIPS’20)

to the size of 299×299 for Inception-V3 and 224×224 for the other three models. Note that we do not pre-process the adversarial images as we discuss input pre-processing as a defense in the evaluation.

Attacks and defenses. For each of the five attack categories presented in Section 3, we select 5 representative attacks (but only 3 for gradient stabilization), resulting in a total number of 23 attacks, as summarized in Table 1. Following the common practice, the L_∞ norm bound is set to $\epsilon = 16/255$. In addition to testing against standard models, we also consider 9 representative defenses from three different categories, as summarized in Table 2. Note that these defenses are not designed against specific (categories of) attacks but is generally applicable. Detailed descriptions and hyperparameter settings of the selected attacks and defenses can be found in Appendix A.

4.2. Evaluation Metrics for Transferability

We measure the attack transferability at both the coarse- and fine-grained levels. At the coarse level, we follow the common practice to measure the (untargeted) attack success rate. Given an attack \mathcal{A} that generates an adversarial image \mathbf{x}'_i for its original image with the true class label y_i , and the target classifier f , the success rate is defined as:

$$\text{Suc}(\mathcal{A}) = \frac{1}{N} \sum_{i=1}^N \mathbf{1}(f(\mathbf{x}'_i) \neq y_i), \quad (1)$$

where N is the size of the test set, and $\mathbf{1}(\cdot)$ is the indicator function. At the fine-grained level, we measure the ranking position p (starting from 1) of the true class label y_i in the prediction list \mathbf{R} of the target classifier [21, 92]:

$$\text{Rank}(\mathcal{A}) = \frac{1}{N} \sum_{i=1}^N \{p | \mathbf{R}_p(\mathbf{x}'_i) = y_i\}. \quad (2)$$

4.3. Evaluation Metrics for Stealthiness

The imperceptibility is measured by a variety of advanced perceptual metrics, such as Root Mean Squared Error (RMSE), Peak Signal-to-Noise Ratio (PSNR), Structural Similarity Index Measure (SSIM) [75], ΔE [47, 99], Learned Perceptual Image Patch Similarity (LPIPS) [97], and Frechet Inception Distance (FID) [65]. Detailed definitions of these metrics can be found in Appendix B. Beyond imperceptibility, we also look into other, finer-grained stealthiness characteristics regarding the perturbation and misclassification (see Section 6.2 for details).

5. Systematic Analyses of Transfer Attacks

In this section, we conduct systematic analyses of the five categories of attacks. In each category, similar attacks are systematically compared along a single dimension with other fairly set factors. In particular, each attack method is implemented with only its core algorithm, although it may integrate other algorithms for achieving better transferability when it was originally proposed. These analyses also help us determine the attack hyperparameter settings required for our comprehensive evaluation in Section 6.

5.1. Analysis of Gradient Stabilization Attacks

Figure 1 (Top) shows the transferability of the three gradient stabilization attacks under various iterations. As can be seen, all three attacks converge very fast, within 10 iterations, since they accumulate gradients with the momentum. However, using more iterations does not improve and may even harm the performance. This finding indicates that in practice, we should early stop such attacks in order to ensure optimal transferability. More specifically, PI and NI perform better than MI due to the use of looking ahead, but NI is better only at the beginning.

The only difference between PI and NI is the maximum number of previous iterations used to look ahead. To figure out the impact of the number of look-ahead iterations, we repeat the experiments with values from 1 (i.e., PI) to 100 (i.e., NI). Figure 1 (Bottom) shows that the performance drops more as more previous iterations are incorporated to look ahead, and the optimal performance is actually

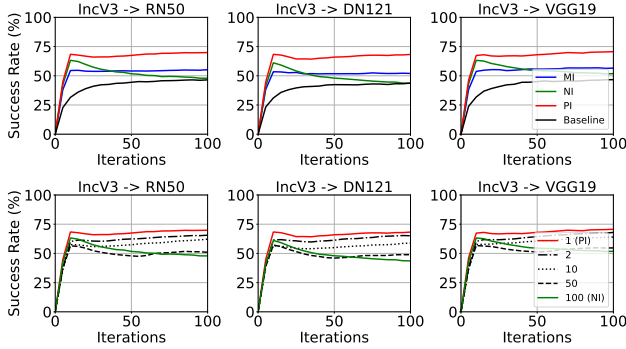


Figure 1. **Results for gradient stabilization attacks. Top:** Transferability for various iterations. **Bottom:** Influence of the number of look-ahead iterations.

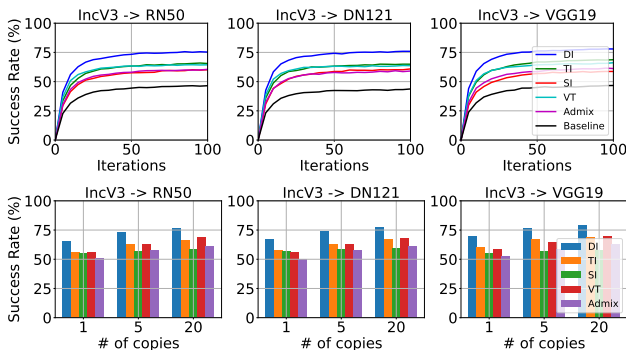


Figure 2. **Results for input augmentation attacks. Top:** Transferability for various iterations. All attacks are implemented with five random copies. **Bottom:** Impact of the number of transformed input copies.

achieved by PI.

5.2. Analysis of Input Augmentation Attacks

Figure 2 (Top) shows the transferability of the five input augmentation attacks for various iterations. Previous evaluations of input augmentation attacks often conduct unfair comparisons because different attacks may leverage a different number of random input copies [73]. Differently, we compare all attacks with the same number of random input copies. Surprisingly, we find that the earliest method, DI, performs the best in all cases. Another early method, TI, often achieves the second-best results.

To further explore the impact of the number of random input copies, we repeat the experiments with various numbers of random input copies. In Figure 2 (Bottom), we see that the transferability of all attacks is improved when more copies are used. In addition, the superiority of DI and TI consistently holds in all settings. This suggests the superiority of spatial transformations (i.e. resizing&padding in DI and translation in TI) over other transformations, such as

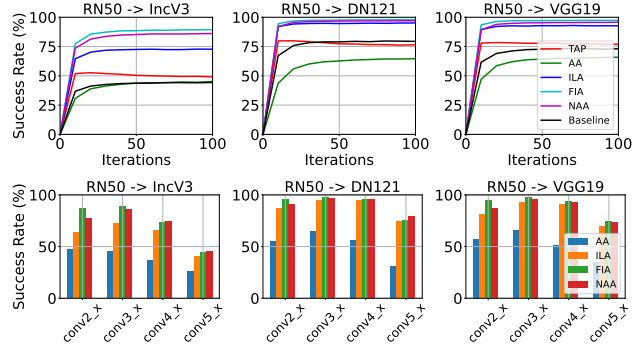


Figure 3. **Results for feature disruption attacks. Top:** Transferability for various iterations. TAP uses all layers and the others use “conv3_x”. **Bottom:** Impact of the layer choice.

pixel scaling in SI, additive noise in VT, and image composition in Admix. Note that more copies generally consume more computational resources.

5.3. Analysis of Feature Disruption Attacks

Figure 3 (Top) shows the transferability of the five feature disruption attacks for various iterations. We see that FIA and NAA, which exploit feature importance, achieve the best results. In addition, ILA and TAP perform well, by incorporating the CE loss into their feature-level optimizations. Finally, AA performs worse than the baseline since it only uses a feature loss.

Since all these attacks, except TAP, only disrupt features in a specific layer, we explore the impact of layer choice. In Figure 3 (Bottom), we see that the last layer (“conv5_x”) performs much worse than the early layers. This might come from the last layer being too complex and model-specific, which results in poor generalizability to unseen models. Moreover, the mid layer (“conv3_x”) always achieves the best performance since it can learn more semantic features but earlier layers normally capture simple features, e.g., colors and textures [90].

5.4. Analysis of Surrogate Refinement Attacks

Figure 4 (Top) shows the transferability of the five surrogate refinement attacks for various iterations. Here ResNet-50 [25] is used as the surrogate model for a fair comparison since SGM [79] can only be applied to architectures with skip connections. We see that IAA achieves the best results since it optimizes the hyperparameters of skip connections and continuous activation functions. In addition, RFA achieves much lower performance (sometimes even lower than the baseline attack) since the standard target and robust surrogate models may rely on distinct features [29].

Model refinement opens a direct way to explore the impact of specific model properties of the surrogate on transferability. Thus we look into model properties in terms of

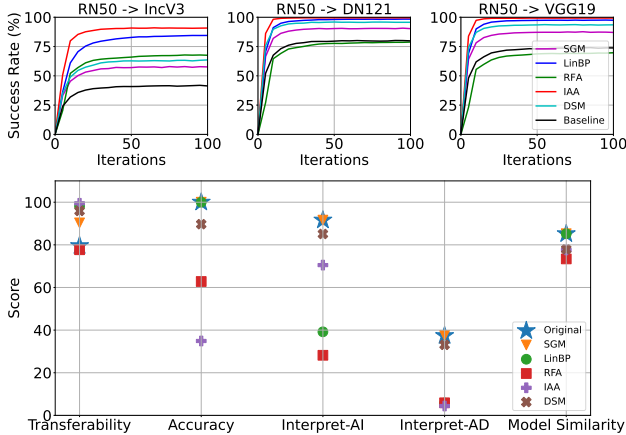


Figure 4. **Results for surrogate refinement attacks.** **Top:** Transferability for various iterations. **Bottom:** Impact of the surrogate property. For all five metrics, higher is better.

two common metrics: accuracy and interpretability, as well as model similarity to the target model. Specifically, interpretability is measured by Average Drop/Increase [10] based on GradCAM [58], and model similarity is measured based on the Kullback-Leibler divergence of output features following [30]. Note that we additionally refine the surrogate models in LinBP and SGM during the forward pass following the same hyperparameters used in backpropagation. Figure 4 (Bottom) shows that there is mostly a negative correlation between the transferability and all the other metrics. Specifically, the accuracy and interpretability results indicate that transferability may be at odds with common model performance. Moreover, the model similarity results indicate that high transferability does not necessarily come from high similarity.

5.5. Analysis of Generative Modeling Attacks

Generative modeling attacks can generate perturbations for any given image with only one forward pass. These perturbations output from the generator are initially unbounded and then clipped to satisfy the imperceptibility. This means that once trained, the generator can be used to generate perturbations under various constraints. Figure 5 (Top) shows the transferability of the five generative modeling attacks under various perturbation bounds. For the targeted attack TTP, we calculate its untargeted transferability over 5000 targeted adversarial images that are generated following the 10-Targets setting [49]. As can be seen, the transferability generally increases as the perturbation constraint is relaxed. It is also worth noting that under strict perturbation constraints, GAPF largely outperforms other attacks, probably due to the use of feature disruptions.

When training the generator, existing work commonly adopts the perturbation bound $\epsilon_{\text{train}} = 10$. For this reason,

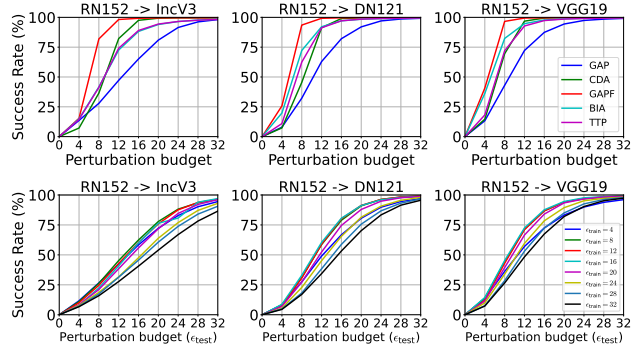


Figure 5. **Results for generative modeling attacks.** **Top:** Transferability for various perturbation budgets. **Bottom:** Impact of the training perturbation bound, for GAP attack.

it is worth exploring the impact of this training perturbation bound on attack transferability. Thus, we re-train the GAP generator with various ϵ_{train} and test these generators across different perturbation bounds ϵ_{test} . Figure 5 (Bottom) shows that adjusting ϵ_{train} has a substantial impact in general. Another unexpected finding is that using the same bound for training and testing (i.e., $\epsilon_{\text{train}} = \epsilon_{\text{test}}$) does not lead to better results, especially when the bound is large. Instead, using a moderate ϵ_{train} (i.e. 8-16) leads to the best results, which also suggests that the commonly used 10 in existing work is indeed optimal.

6. Comprehensive Evaluation Results

In this section, we evaluate all 23 attacks on their transferability against both standard and defended target models, as well as stealthiness regarding diverse metrics. Specifically, for gradient stabilization attacks, we set the iteration number to 10 for early stopping, while for the other three categories of iterative attacks, we set the iteration number to 50 to ensure attack convergence. For input augmentation attacks, we set the number to 5 to offer a good trade-off between performance and computations.

6.1. Transferability Results

Table 3 summarizes the evaluation results in both the standard transfer and defense settings. In general, we find that the optimal performance of one category of attack/defense against one category of defense/attack may not generalize well to another. Moreover, we make the following specific observations.

From the attack perspective: **New model design largely boosts attack performance.** The generative modeling and surrogate refinement attacks, which design new (surrogate or generative) models, achieve the best results in almost all cases, in contrast to the other attacks, which instead use off-of-shelf surrogate models. In particular, IAA performs

Table 3. Attack transferability in terms of success rate (%) / true label ranking. ResNet-50 (ResNet-152 for generative attacks) is used as the backbone architecture of the surrogate model. We also adopt ResNet as the backbone for all defenses to better isolate the specific contribution of defenses from surrogate-target model similarity.

Attacks	Without Defenses			Input Pre-processing			Purification Network			Adversarial Training		
	IncV3	DN121	VGG19	BDR	PD	R&P	HGD	NRP	DiffPure	AT _∞	FD _∞	AT ₂
Clean Acc	100.0	100.0	100.0	89.1	97.3	94.1	98.0/1	90.2	91.7	77.8	81.4	43.2
PGD	43.6/10	79.6/19	72.7/18	100.0/133	100.0/403	98.2/99	84.5/29	78.9/17	13.1/3	22.1/2	18.6/2	61.2/35
MI [17]	55.8/19	85.7/30	78.1/25	100.0/213	100.0/448	98.6/104	87.5/35	49.4/5	21.4/3	22.6/3	18.9/2	64.9/45
NI [42]	60.4/27	87.2/47	82.7/41	100.0/316	100.0/538	99.2/179	88.2/57	<u>83.3/32</u>	20.0/3	22.4/3	19.1/2	64.3/43
PI [74]	66.0/34	92.1/63	87.7/51	100.0/376	100.0/538	99.7/224	81.3/34	93.3/73	20.4/3	22.8/3	19.2/2	64.4/44
DI [84]	69.8/41	99.0/118	99.1/132	100.0/294	100.0/512	100.0/523	98.9/135	81.4/29	16.1/2	22.9/3	19.5/2	62.3/37
TI [18]	63.0/26	96.9/64	96.1/67	100.0/236	100.0/409	100.0/308	97.9/78	78.4/17	16.1/2	22.9/3	19.1/2	62.3/37
SI [42]	61.8/33	93.8/61	85.6/45	100.0/315	100.0/519	99.2/187	95.2/81	72.6/18	14.6/2	22.6/3	19.2/2	62.6/38
VT [72]	67.1/38	95.4/65	92.5/58	100.0/352	100.0/467	99.8/232	97.8/91	80.5/25	19.1/3	22.8/3	19.1/2	63.3/40
Admix [73]	53.4/20	86.7/43	83.5/45	100.0/210	95.3/426	95.0/175	89.9/66	80.0/23	14.1/2	22.7/3	19.0/2	62.1/38
TAP [102]	50.3/21	77.0/69	77.6/61	100.0/740	100.0/777	95.6/229	80.5/87	40.9/8	15.8/3	22.6/3	19.4/2	64.4/45
AA [32]	43.5/20	61.8/43	64.1/42	91.0/167	88.4/153	81.4/107	67.8/64	14.7/2	20.6/4	24.9/3	21.4/3	65.1/47
ILA [27]	72.3/63	94.5/141	92.6/113	100.0/413	100.0/455	99.1/268	94.8/147	<u>83.5/36</u>	18.2/3	22.6/3	19.1/2	63.9/43
FIA [76]	88.4/237	97.5/399	97.1/35	100.0/713	99.9/697	99.6/563	98.1/433	71.6/84	28.5/7	25.1/3	21.3/3	68.2/52
NAA [95]	85.0/123	96.7/215	95.3/17	99.9/454	99.9/480	99.1/328	97.2/240	76.8/46	29.2/5	24.8/3	21.3/2	66.2/45
SGM [79]	57.0/22	90.3/38	87.1/40	90.4/33	100.0/383	97.6/98	94.5/58	83.1/22	14.9/2	22.7/3	18.9/2	62.2/37
LinBP [24]	82.8/164	98.1/284	97.4/267	96.6/217	100.0/662	99.2/397	98.3/316	66.8/36	17.7/3	23.1/3	19.4/2	63.8/41
RFA [63]	66.0/65	77.7/71	68.7/45	81.7/101	80.4/87	77.5/79	72.8/71	21.0/4	69.4/91	62.0/30	53.4/21	87.3/147
IAA [103]	90.8/354	99.5/714	99.2/642	98.9/630	100.0/990	99.9/893	99.9/831	65.4/105	20.6/4	23.0/3	19.5/2	65.5/48
DSM [86]	62.8/38	95.9/101	93.5/89	85.1/40	92.7/68	88.3/60	89.3/69	23.2/2	15.3/2	23.0/3	19.7/2	62.5/38
GAP [54]	65.1/97	82.1/130	87.4/153	85.1/139	87.0/161	83.5/125	93.9/263	2.0/1	16.8/3	21.7/2	18.2/2	64.2/47
CDA [50]	<u>97.8/341</u>	<u>99.2/339</u>	<u>99.2/374</u>	97.6/268	100.0/581	98.3/297	<u>99.9/426</u>	3.9/1	<u>62.0/66</u>	<u>26.0/4</u>	<u>22.6/3</u>	<u>73.2/75</u>
GAPF [34]	99.2/448	99.6/443	99.6/470	99.5/398	99.6/415	99.8/429	<u>99.8/467</u>	14.3/2	28.9/10	23.4/3	20.2/2	67.7/56
BIA [96]	88.2/216	97.1/289	97.8/288	96.9/267	95.4/249	96.6/291	98.7/364	2.6/1	20.0/4	<u>25.3/4</u>	<u>22.2/3</u>	66.7/52
TTP [49]	89.0/247	97.1/293	97.3/327	97.6/307	98.2/331	97.9/327	95.4/263	36.2/17	<u>37.4/20</u>	25.3/3	21.3/3	<u>68.7/60</u>

much better than the other methods in terms of pushing down the ranking positions of the true label since it fundamentally disrupts the data distribution [103]. **Transferring from ResNet50 to Inception-v3 is harder than to other architectures.** This is consistent with previous findings in [30, 31, 100] and might be due to the fact that the Inception architecture contains relatively complex components, e.g., multiple-size convolution and two auxiliary classifiers.

From the defense perspective: **Adversarial training is generally effective but input pre-processing is not.** Both the two L_∞ adversarial training defenses, AT_∞ and FD_∞ , are consistently effective against all attacks except RFA, which uses an adversarially-trained surrogate model for generating robust perturbations. The performance of AT_2 is also not sensitive to the attack method but sub-optimal due to the use of a different, L_2 norm. In contrast, input pre-processing defenses are generally not useful, although they are known to be effective against white-box attacks where the perturbations are much smaller [82, 85]. **Defenses may severely overfit to the type of perturbations that are seen during their optimization.** First, we notice that NRP is very effective in mitigating smooth perturbations (e.g., generative perturbations) but performs much worse against other attacks that generate high-frequency, structured perturbations, see Figure 7 and our GitHub repository for perturbation visualizations. In fact, the NRP purification

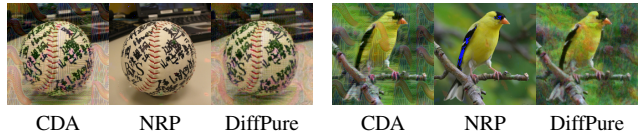


Figure 6. NRP can effectively denoise the CDA perturbations but DiffPure cannot.

network is also trained on relatively smooth perturbations that are optimized in the feature space [48]. Second, DiffPure is originally claimed to provide state-of-the-art white-box robustness [52]. However, we find that surprisingly, black-box transfer attacks (e.g., RFA and CDA) can effectively mitigate DiffPure. This might be because the Gaussian noise used in the diffusion model of DiffPure is not capable of denoising the semantic perturbations generated by RFA and CDA. More generally, our finding suggests that *DiffPure provides a false sense of security and requires a rightful evaluation following recommendations from [2, 8, 69]*. The superiority of NRP over DiffPure in denoising the smooth, CDA perturbations is also confirmed by the visualizations in Figure 6.

6.2. Stealthiness Results

Table 4 reports the imperceptibility results for different attacks following five perceptual metrics. We make the fol-

7. Conclusion

In this paper, we have designed good practices in evaluating transfer adversarial attacks. First, a new attack categorization is proposed to facilitate our systematic and fair analyses of transfer attacks. The analyses also provide interesting observations that complement or even challenge existing knowledge. Furthermore, we present a comprehensive evaluation of 23 representative transfer attacks against 9 defenses on ImageNet. Our extensive evaluation results lead to valuable new insights into both attack transferability and stealthiness. Our work aims to give a thorough picture of the current progress of transfer attacks, and we hope that it can guide future research towards a more meaningful evaluation of transfer adversarial attacks.

8. Acknowledgements

This publication has received funding from the Excellence Initiative of Aix-Marseille Université - A*Midex, a French “Investissements d’Avenir programme” (AMX-21-IET-017), the UnLIR ANR project (ANR-19-CE23-0009), and the CAS Project for Young Scientists in Basic Research (Grant YSBR-040). Part of this work was performed using HPC resources from GENCI-IDRIS (Grant 2020-AD011013110).

References

- [1] Rima Alaifari, Giovanni S Alberti, and Tandri Gauksson. ADef: an iterative algorithm to construct adversarial deformations. In *ICLR*, 2019. 2
- [2] Anish Athalye, Nicholas Carlini, and David Wagner. Obfuscated gradients give a false sense of security: Circumventing defenses to adversarial examples. In *ICML*, 2018. 7
- [3] Anand Bhattad, Min Jin Chong, Kaizhao Liang, Bo Li, and David A Forsyth. Unrestricted adversarial examples via semantic manipulation. In *ICLR*, 2020. 2
- [4] Battista Biggio, Iginio Corona, Davide Maiorca, Blaine Nelson, Nedim Šrđić, Pavel Laskov, Giorgio Giacinto, and Fabio Roli. Evasion attacks against machine learning at test time. In *ECML PKDD*, 2013. 1
- [5] Battista Biggio and Fabio Roli. Wild patterns: Ten years after the rise of adversarial machine learning. *Pattern Recognition*, 84:317–331, 2018. 2
- [6] Wieland Brendel, Jonas Rauber, and Matthias Bethge. Decision-based adversarial attacks: Reliable attacks against black-box machine learning models. In *ICLR*, 2018. 1
- [7] Junyoung Byun, Seungju Cho, Myung-Joon Kwon, Hee-Seon Kim, and Changick Kim. Improving the transferability of targeted adversarial examples through object-based diverse input. In *CVPR*, 2022. 3
- [8] Nicholas Carlini, Anish Athalye, Nicolas Papernot, Wieland Brendel, Jonas Rauber, Dimitris Tsipras, Ian Goodfellow, Aleksander Madry, and Alexey Kurakin. On evaluating adversarial robustness. In *arXiv*, 2019. 2, 7
- [9] Nicholas Carlini and David Wagner. Towards evaluating the robustness of neural networks. In *IEEE S&P*, 2017. 2
- [10] A. Chattopadhyay, A. Sarkar, P. Howlader, and V. N. Balasubramanian. Grad-CAM++: Generalized gradient-based visual explanations for deep convolutional networks. In *WACV*, 2018. 6
- [11] Jianbo Chen, Michael I Jordan, and Martin J Wainwright. Hopskipjumpattack: A query-efficient decision-based attack. In *IEEE S&P*, 2020. 1
- [12] Pin-Yu Chen, Huan Zhang, Yash Sharma, Jinfeng Yi, and Cho-Jui Hsieh. Zoo: Zeroth order optimization based black-box attacks to deep neural networks without training substitute models. In *AISec*, 2017. 1
- [13] Steven Chen, Nicholas Carlini, and David Wagner. Stateful detection of black-box adversarial attacks. In *SPAI*, 2020. 1
- [14] Sizhe Chen, Qinghua Tao, Zhixing Ye, and Xiaolin Huang. Measuring L_∞ attacks by the L_2 norm. In *arXiv*, 2021. 1
- [15] Francesco Croce and Matthias Hein. Sparse and imperceptible adversarial attacks. In *ICCV*, 2019. 2
- [16] Zhun Deng, Linjun Zhang, Kailas Vodrahalli, Kenji Kawaguchi, and James Y Zou. Adversarial training helps transfer learning via better representations. In *NeurIPS*, 2021. 3
- [17] Yinpeng Dong, Fangzhou Liao, Tianyu Pang, Hang Su, Jun Zhu, Xiaolin Hu, and Jianguo Li. Boosting adversarial attacks with momentum. In *CVPR*, 2018. 3, 4, 7, 8, 13, 15
- [18] Yinpeng Dong, Tianyu Pang, Hang Su, and Jun Zhu. Evading defenses to transferable adversarial examples by translation-invariant attacks. In *CVPR*, 2019. 3, 4, 7, 8, 13, 15
- [19] Logan Engstrom, Andrew Ilyas, Hadi Salman, Shibani Santurkar, and Dimitris Tsipras. Robustness (python library). <https://github.com/MadryLab/robustness>, 2019. 14, 15
- [20] Jessica Fridrich. Digital image forensics. *IEEE Signal Processing Magazine*, 2009. 8
- [21] Aditya Ganeshan, Vivek BS, and R Venkatesh Babu. FDA: Feature disruptive attack. In *ICCV*, 2019. 3, 4
- [22] Ian Goodfellow, Jonathon Shlens, and Christian Szegedy. Explaining and harnessing adversarial examples. In *ICLR*, 2015. 2
- [23] Chuan Guo, Jacob Gardner, Yurong You, Andrew Gordon Wilson, and Kilian Weinberger. Simple black-box adversarial attacks. In *ICML*, 2019. 1
- [24] Yiwen Guo, Qizhang Li, and Hao Chen. Backpropagating linearly improves transferability of adversarial examples. In *NeurIPS*, 2020. 3, 4, 7, 8, 13, 15
- [25] Kaiming He, Xiangyu Zhang, Shaoqing Ren, and Jian Sun. Deep residual learning for image recognition. In *CVPR*, 2016. 3, 5
- [26] Gao Huang, Zhuang Liu, Laurens Van Der Maaten, and Kilian Q Weinberger. Densely connected convolutional networks. In *CVPR*, 2017. 3
- [27] Qian Huang, Isay Katsman, Horace He, Zeqi Gu, Serge Be-longie, and Ser-Nam Lim. Enhancing adversarial example transferability with an intermediate level attack. In *ICCV*, 2019. 3, 4, 7, 8, 13, 15

- [28] Andrew Ilyas, Logan Engstrom, Anish Athalye, and Jessy Lin. Black-box adversarial attacks with limited queries and information. In *ICML*, 2018. 1
- [29] Andrew Ilyas, Shibani Santurkar, Dimitris Tsipras, Logan Engstrom, Brandon Tran, and Aleksander Madry. Adversarial examples are not bugs, they are features. In *NeurIPS*, 2019. 5
- [30] Nathan Inkawhich, Kevin Liang, Lawrence Carin, and Yiran Chen. Transferable perturbations of deep feature distributions. In *ICLR*, 2020. 3, 6, 7
- [31] Nathan Inkawhich, Kevin J Liang, Binghui Wang, Matthew Inkawhich, Lawrence Carin, and Yiran Chen. Perturbing across the feature hierarchy to improve standard and strict blackbox attack transferability. In *NeurIPS*, 2020. 3, 7
- [32] Nathan Inkawhich, Wei Wen, Hai Helen Li, and Yiran Chen. Feature space perturbations yield more transferable adversarial examples. In *CVPR*, 2019. 3, 4, 7, 8, 13, 15
- [33] Can Kanbak, Seyed-Mohsen Moosavi-Dezfooli, and Pascal Frossard. Geometric robustness of deep networks: analysis and improvement. In *CVPR*, 2018. 2
- [34] Krishna kanth Nakka and Mathieu Salzmann. Learning transferable adversarial perturbations. In *NeurIPS*, 2021. 3, 4, 7, 8, 14, 15
- [35] Simon Kornblith, Mohammad Norouzi, Honglak Lee, and Geoffrey Hinton. Similarity of neural network representations revisited. In *ICML*, 2019. 3
- [36] Alexey Kurakin, Ian Goodfellow, and Samy Bengio. Adversarial examples in the physical world. In *ICLR*, 2017. 2
- [37] Qizhang Li, Yiwen Guo, and Hao Chen. Yet another intermediate-level attack. In *ECCV*, 2020. 3
- [38] Yingwei Li, Song Bai, Cihang Xie, Zhenyu Liao, Xiaohui Shen, and Alan L Yuille. Regional homogeneity: Towards learning transferable universal adversarial perturbations against defenses. In *ECCV*, 2020. 3
- [39] Yingwei Li, Song Bai, Yuyin Zhou, Cihang Xie, Zhishuai Zhang, and Alan L Yuille. Learning transferable adversarial examples via ghost networks. In *AAAI*, 2020. 3
- [40] Kaizhao Liang, Jacky Y Zhang, Boxin Wang, Zhuolin Yang, Sanmi Koyejo, and Bo Li. Uncovering the connections between adversarial transferability and knowledge transferability. In *ICML*, 2021. 3
- [41] Fangzhou Liao, Ming Liang, Yinpeng Dong, Tianyu Pang, Xiaolin Hu, and Jun Zhu. Defense against adversarial attacks using high-level representation guided denoiser. In *CVPR*, 2018. 4, 14, 15
- [42] Jiadong Lin, Chuanbiao Song, Kun He, Liwei Wang, and John E Hopcroft. Nesterov accelerated gradient and scale invariance for adversarial attacks. In *ICLR*, 2020. 3, 4, 7, 8, 13, 15
- [43] Yanpei Liu, Xinyun Chen, Chang Liu, and Dawn Song. Delving into transferable adversarial examples and black-box attacks. In *ICLR*, 2017. 3
- [44] Zhuoran Liu, Zhengyu Zhao, and Martha Larson. Who’s afraid of adversarial queries? the impact of image modifications on content-based image retrieval. In *ICMR*, 2019. 3
- [45] Yuyang Long, Qilong Zhang, Boheng Zeng, Lianli Gao, Xianglong Liu, Jian Zhang, and Jingkuan Song. Frequency domain model augmentation for adversarial attack. In *ECCV*, 2022. 3
- [46] Bo Luo, Yannan Liu, Lingxiao Wei, and Qiang Xu. Towards imperceptible and robust adversarial example attacks against neural networks. In *AAAI*, 2018. 2
- [47] Ming Ronnier Luo, Guihua Cui, and B. Rigg. The development of the CIE 2000 colour-difference formula: CIEDE2000. *Color Research and Application*, 26:340–350, 2001. 4, 8, 15
- [48] Muzammal Naseer, Salman Khan, Munawar Hayat, Fahad Shahbaz Khan, and Fatih Porikli. A self-supervised approach for adversarial robustness. In *CVPR*, 2020. 4, 7, 14, 15
- [49] Muzammal Naseer, Salman Khan, Munawar Hayat, Fahad Shahbaz Khan, and Fatih Porikli. On generating transferable targeted perturbations. In *ICCV*, 2021. 2, 3, 4, 6, 7, 8, 14, 15
- [50] Muzammal Naseer, Salman H Khan, Harris Khan, Fahad Shahbaz Khan, and Fatih Porikli. Cross-domain transferability of adversarial perturbations. In *NeurIPS*, 2019. 2, 3, 4, 7, 8, 14, 15
- [51] Muzammal Naseer, Salman H Khan, Shafin Rahman, and Fatih Porikli. Task-generalizable adversarial attack based on perceptual metric. In *arXiv*, 2018. 3
- [52] Weili Nie, Brandon Guo, Yujia Huang, Chaowei Xiao, Arash Vahdat, and Anima Anandkumar. Diffusion models for adversarial purification. In *ICML*, 2022. 2, 4, 7, 14, 15
- [53] Nicolas Papernot, Patrick McDaniel, Somesh Jha, Matt Fredrikson, Z Berkay Celik, and Ananthram Swami. The limitations of deep learning in adversarial settings. In *EuroS&P*, 2016. 2
- [54] Omid Poursaeed, Isay Katsman, Bicheng Gao, and Serge Belongie. Generative adversarial perturbations. In *CVPR*, 2018. 3, 4, 7, 8, 13, 15
- [55] Aaditya Prakash, Nick Moran, Solomon Garber, Antonella DiLillo, and James Storer. Deflecting adversarial attacks with pixel deflection. In *CVPR*, 2018. 4, 14, 15
- [56] Andras Rozsa, Ethan M Rudd, and Terrance E Boult. Adversarial diversity and hard positive generation. In *CVPRW*, 2016. 2
- [57] Hadi Salman, Andrew Ilyas, Logan Engstrom, Ashish Kapoor, and Aleksander Madry. Do adversarially robust imagenet models transfer better? In *NeurIPS*, 2020. 3, 4
- [58] Ramprasaath R Selvaraju, Michael Cogswell, Abhishek Das, Ramakrishna Vedantam, Devi Parikh, and Dhruv Batra. Grad-cam: Visual explanations from deep networks via gradient-based localization. In *ICCV*, 2017. 3, 6
- [59] Ali Shahin Shamsabadi, Ricardo Sanchez-Matilla, and Andrea Cavallaro. ColorFool: Semantic adversarial colorization. In *CVPR*, 2020. 2
- [60] Mahmood Sharif, Lujo Bauer, and Michael K. Reiter. On the suitability of L_p -norms for creating and preventing adversarial examples. In *CVPRW*, 2018. 1

- [61] Karen Simonyan and Andrew Zisserman. Very deep convolutional networks for large-scale image recognition. In *ICLR*, 2015. 3
- [62] Gowthami Somepalli, Liam Fowl, Arpit Bansal, Ping Yeh-Chiang, Yehuda Dar, Richard Baraniuk, Micah Goldblum, and Tom Goldstein. Can neural nets learn the same model twice? investigating reproducibility and double descent from the decision boundary perspective. In *CVPR*, 2022. 3
- [63] Jacob M Springer, Melanie Mitchell, and Garrett T Kenyon. A little robustness goes a long way: Leveraging robust features for targeted transfer attacks. In *NeurIPS*, 2021. 3, 4, 7, 8, 13, 15
- [64] Mukund Sundararajan, Ankur Taly, and Qiqi Yan. Axiomatic attribution for deep networks. In *ICML*, 2017. 3
- [65] Christian Szegedy, Vincent Vanhoucke, Sergey Ioffe, Jon Shlens, and Zbigniew Wojna. Rethinking the inception architecture for computer vision. In *CVPR*, 2016. 3, 4, 8, 15
- [66] Christian Szegedy, Wojciech Zaremba, Ilya Sutskever, Joan Bruna, Dumitru Erhan, Ian Goodfellow, and Rob Fergus. Intriguing properties of neural networks. In *ICLR*, 2014. 1
- [67] Christian Szegedy, Wojciech Zaremba, Ilya Sutskever, Joan Bruna, Dumitru Erhan, Ian Goodfellow, and Rob Fergus. Intriguing properties of neural networks. In *ICLR*, 2014. 2
- [68] Florian Tramèr, Jens Behrmann, Nicholas Carlini, Nicolas Papernot, and Jörn-Henrik Jacobsen. Fundamental trade-offs between invariance and sensitivity to adversarial perturbations. In *ICML*, 2020. 1
- [69] Florian Tramèr, Nicholas Carlini, Wieland Brendel, and Aleksander Madry. On adaptive attacks to adversarial example defenses. In *NeurIPS*, 2020. 2, 7
- [70] Florian Tramèr, Alexey Kurakin, Nicolas Papernot, Ian Goodfellow, Dan Boneh, and Patrick McDaniel. Ensemble adversarial training: Attacks and defenses. In *ICLR*, 2018. 1
- [71] Francisco Utrera, Evan Kravitz, N Benjamin Erichson, Rajiv Khanna, and Michael W Mahoney. Adversarially-trained deep nets transfer better: Illustration on image classification. In *ICLR*, 2021. 3
- [72] Xiaosen Wang and Kun He. Enhancing the transferability of adversarial attacks through variance tuning. In *CVPR*, 2021. 3, 4, 7, 8, 13, 15
- [73] Xiaosen Wang, Xuanran He, Jingdong Wang, and Kun He. Admix: Enhancing the transferability of adversarial attacks. In *ICCV*, 2021. 3, 4, 5, 7, 8, 13, 15
- [74] Xiaosen Wang, Jiadong Lin, Han Hu, Jingdong Wang, and Kun He. Boosting adversarial transferability through enhanced momentum. In *BMVC*, 2021. 3, 4, 7, 8, 13, 15
- [75] Zhou Wang, Alan C. Bovik, Hamid R. Sheikh, and Eero P. Simoncelli. Image quality assessment: from error visibility to structural similarity. *IEEE Transactions On Image Processing*, 13:600–612, 2004. 4, 8, 14
- [76] Zhibo Wang, Hengchang Guo, Zhifei Zhang, Wenxin Liu, Zhan Qin, and Kui Ren. Feature importance-aware transferable adversarial attacks. In *ICCV*, 2021. 3, 4, 7, 8, 13, 15
- [77] Zhipeng Wei, Jingjing Chen, Zuxuan Wu, and Yu-Gang Jiang. Incorporating locality of images to generate targeted transferable adversarial examples. In *arXiv*, 2022. 3
- [78] Eric Wong, Frank Schmidt, and Zico Kolter. Wasserstein adversarial examples via projected sinkhorn iterations. In *ICML*, 2019. 2
- [79] Dongxian Wu, Yisen Wang, Shu-Tao Xia, James Bailey, and Xingjun Ma. Skip connections matter: On the transferability of adversarial examples generated with ResNets. In *ICLR*, 2020. 3, 4, 5, 7, 8, 13, 15
- [80] Weibin Wu, Yuxin Su, Xixian Chen, Shenglin Zhao, Irwin King, Michael R Lyu, and Yu-Wing Tai. Boosting the transferability of adversarial samples via attention. In *CVPR*, 2020. 3
- [81] Chaowei Xiao, Jun-Yan Zhu, Bo Li, Warren He, Mingyan Liu, and Dawn Song. Spatially transformed adversarial examples. In *ICLR*, 2018. 2
- [82] Cihang Xie, Jianyu Wang, Zhishuai Zhang, Zhou Ren, and Alan Yuille. Mitigating adversarial effects through randomization. In *ICLR*, 2018. 4, 7, 14, 15
- [83] Cihang Xie, Yuxin Wu, Laurens van der Maaten, Alan L Yuille, and Kaiming He. Feature denoising for improving adversarial robustness. In *CVPR*, 2019. 4, 14, 15
- [84] Cihang Xie, Zhishuai Zhang, Yuyin Zhou, Song Bai, Jianyu Wang, Zhou Ren, and Alan L Yuille. Improving transferability of adversarial examples with input diversity. In *CVPR*, 2019. 2, 3, 4, 7, 8, 13, 15
- [85] Weilin Xu, David Evans, and Yanjun Qi. Feature squeezing: Detecting adversarial examples in deep neural networks. In *NDSS*, 2018. 4, 7, 14, 15
- [86] Dingcheng Yang, Zihao Xiao, and Wenjian Yu. Boosting the adversarial transferability of surrogate model with dark knowledge. In *arXiv*, 2022. 3, 4, 7, 8, 13, 15
- [87] Xiao Yang, Yinpeng Dong, Tianyu Pang, Hang Su, and Jun Zhu. Boosting transferability of targeted adversarial examples via hierarchical generative networks. In *ECCV*, 2022. 3
- [88] Jason Yosinski, Jeff Clune, Yoshua Bengio, and Hod Lipson. How transferable are features in deep neural networks? In *NeurIPS*, 2014. 3
- [89] Zheng Yuan, Jie Zhang, and Shiguang Shan. Adaptive image transformations for transfer-based adversarial attack. In *ECCV*, 2022. 3
- [90] Matthew D Zeiler and Rob Fergus. Visualizing and understanding convolutional networks. In *ECCV*, 2014. 5
- [91] Chaoning Zhang, Philipp Benz, Gyusang Cho, Adil Karjauv, Soomin Ham, Chan-Hyun Youn, and In So Kweon. Backpropagating smoothly improves transferability of adversarial examples. In *CVPR Workshop on AML*, 2021. 3
- [92] Chaoning Zhang, Philipp Benz, Adil Karjauv, Jae Won Cho, Kang Zhang, and In So Kweon. Investigating top-k white-box and transferable black-box attack. In *CVPR*, 2022. 4
- [93] Chaoning Zhang, Gyusang Cho, Philipp Benz, Kang Zhang, Chenshuang Zhang, Chan-Hyun Youn, and In So Kweon. Early stop and adversarial training yield better surrogate model: Very non-robust features harm adversarial transferability. In *OpenReview*, 2021. 3

- [94] Hanwei Zhang, Yannis Avrithis, Teddy Furon, and Laurent Amsaleg. Smooth adversarial examples. *EURASIP Journal on Information Security*, 2020. 2
- [95] Jianping Zhang, Weibin Wu, Jen-tse Huang, Yizhan Huang, Wenxuan Wang, Yuxin Su, and Michael R Lyu. Improving adversarial transferability via neuron attribution-based attacks. In *CVPR*, 2022. 3, 4, 7, 8, 13, 15
- [96] Qilong Zhang, Xiaodan Li, Yuefeng Chen, Jingkuan Song, Lianli Gao, Yuan He, and Hui Xue. Beyond imagenet attack: Towards crafting adversarial examples for black-box domains. In *ICLR*, 2022. 2, 3, 4, 7, 8, 14, 15
- [97] Richard Zhang, Phillip Isola, Alexei A Efros, Eli Shechtman, and Oliver Wang. The unreasonable effectiveness of deep features as a perceptual metric. In *CVPR*, 2018. 4, 8, 15
- [98] Zhengyu Zhao, Zhuoran Liu, and Martha Larson. Adversarial image color transformations in explicit color filter space. In *arXiv*, 2020. 2
- [99] Zhengyu Zhao, Zhuoran Liu, and Martha Larson. Towards large yet imperceptible adversarial image perturbations with perceptual color distance. In *CVPR*, 2020. 2, 4, 8, 15
- [100] Zhengyu Zhao, Zhuoran Liu, and Martha Larson. On success and simplicity: A second look at transferable targeted attacks. In *NeurIPS*, 2021. 2, 7
- [101] Bolei Zhou, Aditya Khosla, Agata Lapedriza, Aude Oliva, and Antonio Torralba. Learning deep features for discriminative localization. In *CVPR*, 2016. 3
- [102] Wen Zhou, Xin Hou, Yongjun Chen, Mengyun Tang, Xiangqi Huang, Xiang Gan, and Yong Yang. Transferable adversarial perturbations. In *ECCV*, 2018. 3, 4, 7, 8, 13, 15
- [103] Yao Zhu, Jiacheng Sun, and Zhenguo Li. Rethinking adversarial transferability from a data distribution perspective. In *ICLR*, 2022. 3, 4, 7, 8, 13, 15
- [104] Junhua Zou, Zhisong Pan, Junyang Qiu, Xin Liu, Ting Rui, and Wei Li. Improving the transferability of adversarial examples with resized-diverse-inputs, diversity-ensemble and region fitting. In *ECCV*, 2020. 3

A. Descriptions of Attacks and Defenses

A.1. Descriptions of Attacks

Momentum Iterative (MI) [17] integrates the momentum term into the iterative optimization of attacks, in order to stabilize the update directions and escape from poor local maxima. This momentum term accumulates a velocity vector in the gradient direction of the loss function across iterations.

Nesterov Iterative (NI) [42] is based on an improved momentum method that further also leverages the look ahead property of Nesterov Accelerated Gradient (NAG) by making a jump in the direction of previously accumulated gradients before computing the gradients in the current iteration. This makes the attack escape from poor local maxima more easily and faster.

Pre-gradient guided Iterative (PI) [74] follows a similar idea as NI, but it makes a jump based on only the gradients from the last iteration instead of all previously accumulated gradients.

Diverse Inputs (DI) [84] applies random image resizing and padding to the input image before calculating the gradients in each iteration of the attack optimization. This approach aims to prevent attack overfitting (to the white-box, source model), inspired by the data augmentation techniques used for preventing model overfitting.

Translation Invariant (TI) [18] applies random image translations for input augmentation. It also introduces an approximate solution to improve the attack efficiency by directly computing locally smoothed gradients on the original image through the convolution operations rather than computing gradients multiple times for all potential translated images.

Scale Invariant (SI) [42] applies random image scaling for input augmentation. It scales pixels with a factor of $1/2^i$. In particular, in each iteration, it takes an average of gradients on multiple augmented images rather than using only one augmented image as in previous input augmentation attacks.

Variance Tuning (VT) [72] applies uniformly distributed additive noise to images for input augmentation and also calculates average gradients over multiple augmented images in each iteration.

Adversarial mixup (Admix) [73] calculates the gradients on a composite image that is made up of the original image and another image randomly selected from an incorrect class. The original image label is still used in the loss function.

Transferable Adversarial Perturbations (TAP) [102] proposes to maximize the distance between original images and their adversarial examples in the intermediate feature space and also introduces a regularization term for reducing the variations of the perturbations and another regulariza-

tion term with the cross-entropy loss.

Activation Attack (AA) [32] drives the feature-space representation of the original image towards the representation of a target image that is selected from another class. Specifically, AA can achieve targeted misclassification by selecting a target image from that specific target class.

Intermediate Level Attack (ILA) [27] optimizes the adversarial examples in two stages, with the cross-entropy loss used in the first stage to determine the initial perturbations, which will be further fine-tuned in the second stage towards larger feature distance while maintaining the initial perturbation directions.

Feature Importance-aware Attack (FIA) [76] proposes to only disrupts important features. Specifically, it measures the importance of features based on the aggregated gradients with respect to feature maps computed on a batch of transformed original images that are achieved by random image masking.

Neuron Attribution-based Attacks (NAA) [95] relies on an advanced neuron attribution method to measure the feature importance more accurately. It also introduces an approximation approach to conducting neuron attribution with largely reduced computations.

Skip Gradient Method (SGM) [79] suggests using ResNet-like architectures as the source model during creating the adversarial examples. Specifically, it shows that backpropagating gradients through skip connections lead to higher transferability than through the residual modules.

Linear BackPropagation (LinBP) [24] is proposed based on the new finding that the non-linearity of the commonly used ReLU activation function substantially limits the transferability. To address this limitation, the ReLU is replaced by a linear function during only the backpropagation process.

Robust Feature-guided Attack (RFA) [63] proposes to use an adversarially-trained model as the source model based on the assumption that modifying more robust features yields more generalizable (transferable) adversarial examples.

Intrinsic Adversarial Attack (IAA) [103] finds that disturbing the intrinsic data distribution is the key to generating transferable adversarial examples. Based on this, it optimizes the hyperparameters of the Softplus and the weights of skip connections per layer towards aligned attack directions and data distribution.

Dark Surrogate Model (DSM) [86] is trained from scratch with additional “dark” knowledge, which is achieved by training with soft labels from a pre-trained teacher model and using data augmentation techniques, such as Cutout, Mixup, and CutMix.

Generative Adversarial Perturbations (GAP) [54] proposes a new attack approach that is based on generative modeling. Specifically, it uses the source classifier as the

discriminator and trains a generator using the cross-entropy loss. Once trained, the generator can be used to generate an adversarial example for each input original image with only one forward pass.

Cross-Domain Attack (CDA) [50] follows the GAP pipeline but uses a more advanced loss (i.e., relativistic cross entropy) to train the generator. This new loss explicitly enforces the probability gap between the clean and adversarial images, boosting the transferability, especially in cross-domain scenarios.

Transferable Targeted Perturbations (TTP) [49] is focused on improving transferability of targeted attacks. It is based on learning target-specific generators, each of which is trained with the objective of matching the distribution of targeted perturbations with that of data from a specific target class. Specifically, input augmentation and smooth perturbation projection are used to further boost the performance.

Generative Adversarial Feature Perturbations (GAFFP) [34] follows the general pipeline of GAP but trains the generator using a loss that maximizes the feature map distance between adversarial and original images at mid-level CNN layers.

Beyond ImageNet Attack (BIA) [96] also follows the general pipeline of GAP and specifically introduces a random normalization module to simulate different training data distributions and also a feature distance loss that is only based on important/generalizable features.

A.2. Descriptions of Defenses

Bit-Depth Reduction (BDR) [85] pre-processes input images by reducing the color depth of each pixel while maintaining the semantics. This operation can eliminate pixel-level adversarial perturbations from adversarial images but have little impact on model predictions of clean images.

Pixel Deflection (PD) [55] pre-processes input images by randomly replacing some pixels with randomly selected pixels from their local neighborhood. It is specifically designed to happen more frequently to non-salient pixels, and a subsequent wavelet-based denoising operation is used to soften the corruption.

Resizing and Padding (R&P) [82] pre-processes input images by random resizing, which resizes the input images to a random size, and then random padding, which pads zeros around the resized input images.

High-level representation Guided Denoiser (HGD) [41] learns a purification network that can be used to purify/denoise the adversarial perturbations. Specifically, different from previous methods that focus on image-space denoising, HGD minimizes the difference between the clean image and the denoised image at intermediate feature layers.

Neural Representation Purifier (NRP) [48] learns a purification network using a combined loss that calculates

both the image- and feature-space differences. Specifically, the adversarial images used for training the purification network are generated by feature loss-based adversaries, which are shown to be more effective in handling unseen attacks.

Diffusion Purification (DiffPure) [52] uses a diffusion model as the purification network. It diffuses an input image by gradually adding noise in a forward diffusion process and then recovers the clean image by gradually denoising the image in a reverse generative process. The reverse process is shown to be also capable of removing adversarial perturbations.

L_∞ -Adversarial Training (AT $_\infty$) [83] follows the basic pipeline of adversarial training, which is to train the robust model on adversarial images. Specifically, these adversarial images are generated using the PGD targeted attacks with the L_∞ distance, and the model is trained distributedly on 128 Nvidia V100 GPUs.

L_∞ -Adversarial Training with Feature Denoising (FD $_\infty$) [83] modifies the standard model architecture by introducing new building blocks that are designed for denoising feature maps based on non-local means or other filters. This modification can help suppress the potential disruptions caused by the adversarial perturbations, and the modified model is trained end-to-end.

L_2 -Adversarial Training (AT $_2$) [19] trains the model on adversarial images that are generated using the PGD non-targeted attacks with the L_2 distance.

A.3. Hyperparameter Settings

The hyperparameter settings adopted in our evaluation for the attacks and defenses are described in Table 5.

B. Definitions of Imperceptibility Metrics

Peak Signal-to-Noise Ratio (PSNR) measures the ratio of the maximum possible power of a signal (image x) to the noise (perturbations σ) power. It is calculated by:

$$\text{PSNR}(x, \sigma) = 10 \cdot \log_{10} \frac{\max(x)^2}{\text{MSE}(x, \sigma)}, \quad (3)$$

where the Mean Squared Error (MSE) measures the average squared difference between the two inputs.

Structural Similarity Index Measure (SSIM) [75] is used for measuring the perceptual quality of digital images. In our case, it measures the structural similarity between the original image x and adversarial image x' , which is considered to be a degraded version of x . It is calculated by:

$$\text{SSIM}(x, x') = \frac{(2\mu_x\mu_{x'} + c_1) + (2\sigma_{xx'} + c_2)}{(\mu_x^2 + \mu_{x'}^2 + c_1)(\sigma_x^2 + \sigma_{x'}^2 + c_2)}. \quad (4)$$

Descriptions of c_1 and c_1 and more technical details can be found in [75].

Table 5. Hyperparameter settings of attacks and defenses.

Attacks	Hyperparameter settings
MI [17]	decay factor $\mu = 1$
NI [42]	decay factor $\mu = 1$
PI [74]	decay factor $\mu = 1$
DI [84]	resize&pad range $R = [1, 1.1]$
TI [18]	transformation probability $p = 0.7$
SI [42]	translation range $R = [-2, 2]$
VT [72]	scale range $R = [0.1, 1]$
Admix [73]	noise range $R = [-1.5\epsilon, 1.5\epsilon]$
TAP [102]	mixing factor $\eta = 0.2$
AA [32]	$\lambda = 0.005, \eta = 0.01, \alpha = 0.5$
ILA [27]	20 random target images from 4 classes
FIA [76]	ILA projection loss
NAA [95]	$N = 30, P_{\text{drop}} = 0.3$
SGM [79]	$N = 30, \gamma = 1.0$, linear transformation
LinBP [24]	decay parameter $\gamma = 0.5$
RFA [63]	first residual unit in the third meta block
IAA [103]	$L_\infty \epsilon = 8$ PGD-AT, ResNet50
DSM [86]	$\beta = 15$, ResNet50
GAP [54]	Cutout augmentation, ResNet18
CDA [50]	ResNet152 discriminator
GAPF [34]	ResNet152 discriminator
BIA [96]	ResNet152 discriminator, RN module
TTP [49]	ResNet50 discriminator
Defenses	Hyperparameter settings
BDR [85]	bit depth $D = 2$
PD [55]	R-CAM: $k = 5$, denoising: $\sigma = 0.04$
R&P [82]	resize&pad range $R = [1, 1.1]$
HGD [41]	ResNet152-Wide
NRP [48]	ResNet (1.2M parameters)
DiffPure [52]	noise level $t = 150$ WideResNet-50-2
AT $_\infty$ [83]	$L_\infty \epsilon = 16$, PGD iters $n = 30$, lr= $\alpha = 1$
FD $_\infty$ [83]	$L_\infty \epsilon = 16$, PGD iters $n = 30$, lr= $\alpha = 1$
AT $_2$ [19]	$L_2 \epsilon = 3.0$, PGD iters $n = 7$, lr= $\alpha = 0.5$

ΔE [47] refers to the CIE ΔE standard formula used for measuring the perceptual color distance between two pixels. We follow [99] to use the latest variant, CIEDE2000, since it is shown to align very well with human perception. It is calculated in the CIELCH space by:

$$\Delta E = \sqrt{\left(\frac{\Delta L'}{k_L S_L}\right)^2 + \left(\frac{\Delta C'}{k_C S_C}\right)^2 + \left(\frac{\Delta H'}{k_H S_H}\right)^2} + \Delta R, \quad (5)$$

$$\Delta R = R_T \left(\frac{\Delta C'}{k_C S_C}\right) \left(\frac{\Delta H'}{k_H S_H}\right),$$

where $\Delta L'$, $\Delta C'$, $\Delta H'$ denotes the distance between two pixels in their lightness, chroma and hue channels, respectively. ΔR is an interactive term between chroma and hue differences. Detailed definitions and explanations of the

weighting functions (S_L, S_C, S_H and R_T) and hyperparameters k_L, k_C and k_H can be found in [47]. Further, Image-level perceptual color difference is obtained by computing the L_2 norm of the above ΔE for each pixel.

Learned Perceptual Image Patch Similarity (LPIPS) [97] is developed for measuring the perceptual similarity between two images. It computes the cosine distance (in the channel dimension) between features at each given convolutional layer l and averages the results across spatial dimensions $H \times W$ and layers of a specific network f :

$$\text{LPIPS} = \sum_l \frac{1}{H_l W_l} \sum_{h,w} \cos(f_{hw}^l(\mathbf{x}), f_{hw}^l(\mathbf{x}')), \quad (6)$$

where AlexNet is adopted as f for computational efficiency. **Fréchet Inception Distance (FID)** [65] is originally used to assess the quality of images generated by a generative model and can also be used to assess the quality of adversarial images. It compares the distribution of adversarial images to that of original images. Specifically, the output features from the pool3 layer of an Inception-V3 for original and adversarial images are used to fit two multidimensional Gaussian distributions $\mathcal{N}(\mu, \Sigma)$ and $\mathcal{N}(\mu', \Sigma')$, and the FID is score is calculated by:

$$\text{FID}(\mathcal{N}(\mu, \Sigma), \mathcal{N}(\mu', \Sigma')) = \|\mu - \mu'\|_2^2 + \text{tr}(\Sigma + \Sigma' - 2\sqrt{\Sigma \Sigma'}), \quad (7)$$

where tr denotes the trace of the matrix.

C. Additional Results

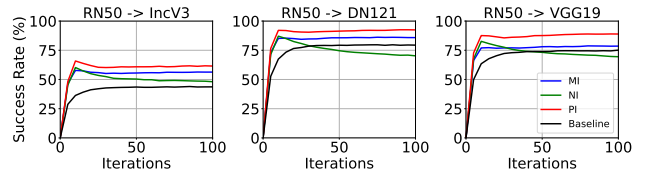


Figure 10. Transferability of gradient stabilization attacks.

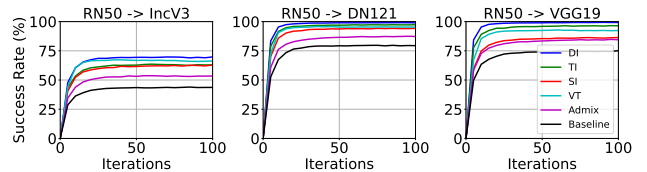


Figure 11. Transferability of input augmentation attacks.

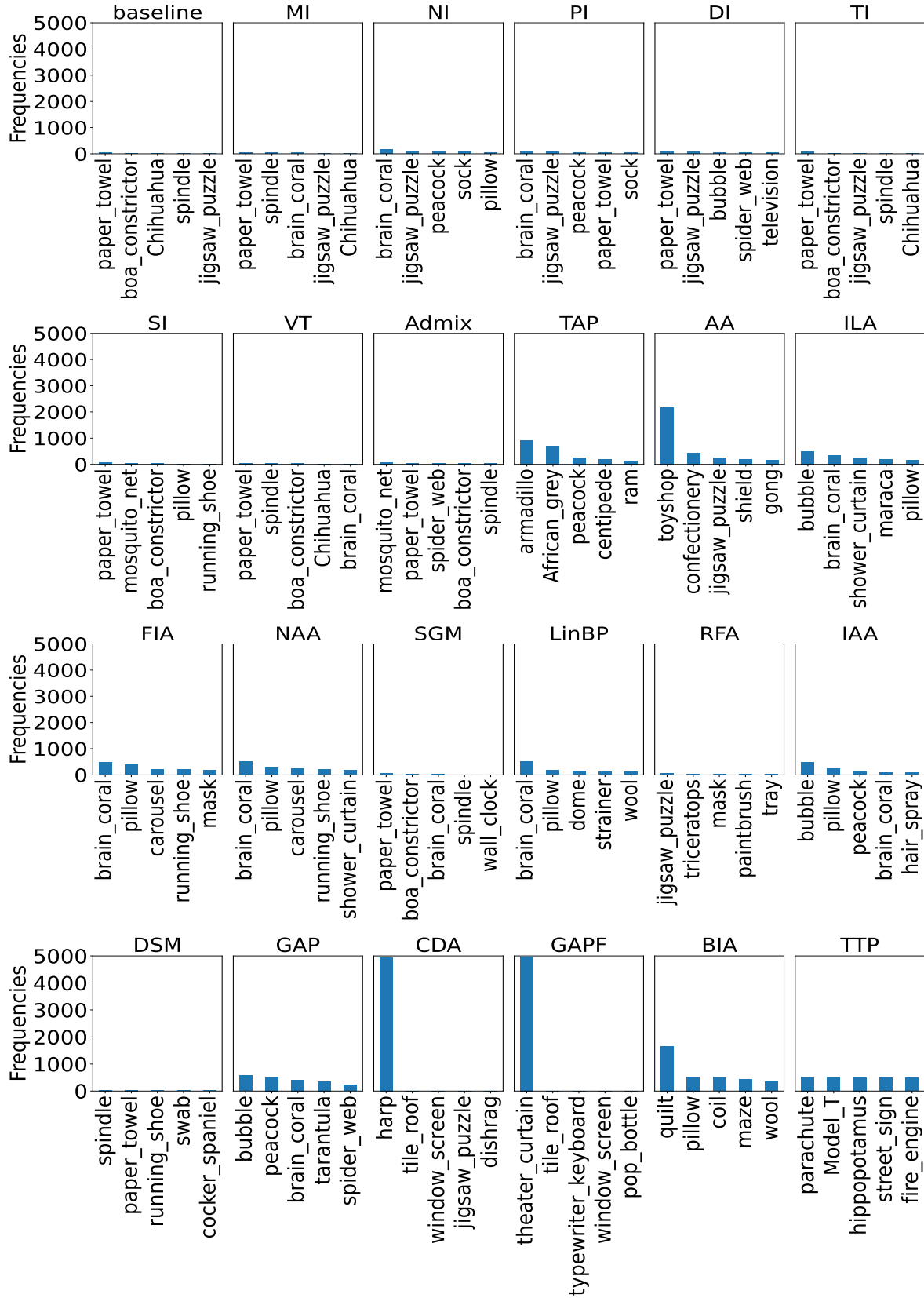


Figure 12. Top-5 frequent class predictions calculated over 5000 adversarial images for different attacks.